

# THE CALIBRATION OF THE O/H ABUNDANCE INDICATORS FOR EXTRAGALACTIC H II REGIONS BASED ON O II RECOMBINATION LINES

M. Peimbert<sup>1</sup>, A. Peimbert<sup>1</sup>, C. Esteban<sup>2</sup>, J. García-Rojas<sup>2</sup>, F. Bresolin<sup>3</sup>, L. Carigi<sup>1</sup>, M. T. Ruiz<sup>4</sup>, and A. R. López-Sánchez<sup>2</sup>

## RESUMEN

Presentamos una nueva calibración del indicador  $O_{23}$  de Pagel para determinar los cocientes de O/H en regiones H II extragalácticas y galaxias con líneas de emisión. Esta calibración la llamamos O II<sub>RL</sub> y esta basada en líneas de recombinación de O II. Nuestra calibración produce abundancias de O/H alrededor de un factor de dos mayores que las obtenidas a partir del método  $T_e(4363)$  con  $t^2 = 0.00$ . La calibración O II<sub>RL</sub> tiene implicaciones para el estudio de diferentes propiedades de las galaxias con líneas de emisión tales como la metalicidad, la tasa de formación estelar, y la función inicial de masas. La calibración O II<sub>RL</sub> también afecta aquellas determinaciones de abundancias basadas en otros indicadores de O/H, que incluyen líneas excitadas colisionalmente, tales como los llamados  $O_3N_2$ ,  $N_2$ ,  $S_{23}$ ,  $Ar_3O_3$ , y  $S_3O_3$ . Argumentamos que la controversia entre el método  $T(4363)$  y el método basado en modelos de fotoionización para determinar O/H se debe principalmente a la presencia de variaciones de temperatura dentro de las regiones H II observadas.

## ABSTRACT

Based on O II recombination lines we present a new calibration (called O II<sub>RL</sub>) of Pagel’s  $O_{23}$  indicator to determine the O/H abundance ratio in extragalactic H II regions and emission line galaxies. The O II<sub>RL</sub> calibration produces O/H abundances about a factor of two higher than those derived from the  $T(4363)$  method with  $t^2 = 0.00$ . The O II<sub>RL</sub> calibration has implications for the study of different properties of emission line galaxies such as their metallicity, star formation rate, and initial mass function. The O II<sub>RL</sub> calibration also affects the abundance determinations based on other O/H indicators, that include collisionally excited lines, like those known as  $O_3N_2$ ,  $N_2$ ,  $S_{23}$ ,  $Ar_3O_3$ , and  $S_3O_3$ . We argue that the controversy between the  $T(4363)$  method and the photoionization models method to derive O/H values is mainly due to temperature variations inside the observed H II regions.

*Key Words:* GALAXIES: ABUNDANCES — H II REGIONS: ABUNDANCES

## 1. INTRODUCTION

The advent of large telescopes is permitting to observe H II regions in galaxies many tens of megaparsecs away from us and emission line galaxies up to distances of  $z \sim 3$ . But since the amount of photons that we obtain from faraway objects is small, often we have reliable information only for a few bright emission lines which has led to the idea of using different metallicity indicators based on at most a handful of bright emission lines.

The most popular metallicity indicator was introduced by Pagel et al. (1979, see also Edmunds & Pagel 1984) and is indistinctly known as Pagel’s, or  $R_{23}$ , or  $O_{23}$  indicator, where  $O_{23} \equiv$

$I([\text{O II}]\lambda 3727 + [\text{O III}]\lambda\lambda 4959, 5007)/I(\text{H}\beta)$ . The  $O_{23}$  indicator has been calibrated with the O/H values based on two different methods: by using photoionization models, that we will call *PIM* calibrations or *PIM* method, and by using observational determinations of the O/H abundances based on the electron temperature derived from the  $I(4363)/I(5007)$  [O III] ratio together with the  $I(3727)/I(\text{H}\beta)$  and the  $I(5007)/I(\text{H}\beta)$  line ratios, the so called  $T(4363)$  method.

There are significant differences between the calibrations of Pagel’s indicator based on models (e. g. McCall et al. 1985; Dopita & Evans 1986; McGaugh 1991; Koblunicky & Kewley 2004) and the calibrations based on observations and  $T(4363)$  (e. g. Torres-Peimbert, Peimbert, & Fierro 1989; Pilyugin 2000, 2003; Castellanos, Díaz, & Terlevich 2002; Pilyugin, & Thuan 2005). The differences in the O/H values are in the 0.2 - 0.6 dex range and could be

<sup>1</sup>Instituto de Astronomía, U.N.A.M. México, D.F., México.

<sup>2</sup>Instituto de Astrofísica de Canarias, Tenerife España.

<sup>3</sup>Institute for Astronomy, University of Hawaii, Honolulu, Hawaii, U.S.A.

<sup>4</sup>Departamento de Astronomía, Universidad de Chile, Chile.

due mainly to the presence of temperature inhomogeneities over the observed volume (e. g. Campbell 1988; Torres-Peimbert et al. 1989; McGaugh 1991; Roy et al. 1996; Luridiana et al. 1999; Kobulnicky, Kennicutt, & Pizagno 1999; Kobulnicky, & Kewley 2004). These differences need to be sorted out if we want to obtain absolute accuracies in O/H of the order of 0.1 dex or better. We will call these differences the calibration controversy.

In this paper we present a qualitatively different calibration of the  $O_{23}$  indicator that is based on the intensity ratio of O II recombination lines to H I recombination lines, that we will call the O II<sub>RL</sub> method. As of now the O II<sub>RL</sub> calibration has been established only for objects in the high metallicity branch of the  $O_{23}$  versus O/H relation and for  $\log O_{23} > 0.5$ .

Preliminary discussions of the O II<sub>RL</sub> calibration were presented by Peimbert & Peimbert (2003, 2005).

## 2. THE $O_{23}$ INDICATOR

The oxygen abundance by unit mass is an excellent tracer of the heavy element content  $Z$  of a given H II region because for extremely poor objects O constitutes about 60% of the heavy elements by mass, while for the present value of the ISM of the solar vicinity it amounts to 43%. In the Local Group galaxies for a metallicity range of  $0.00319 < Z < 0.01990$  (that corresponds to  $8.15 < 12 + \log O/H < 8.86$ ), the fraction of  $Z$  due to O varies from 53% to 41%, mainly due to the increase of N and C relative to O as  $Z$  increases (Peimbert 2003).

There are three different types of methods to calibrate the  $O_{23}$  indicator: a) the *PIM* method, b) the  $T(4363)$  method, and c) the O II<sub>RL</sub> method. We will discuss these three methods and the causes for the O/H differences among them. In particular we will address the calibration controversy: why is it that the calibrations based on the  $T(4363)$  method yield abundances from 0.2 to 0.4 dex lower than the calibrations based on photoionization models in the  $O_{23}$  high metallicity branch for  $\log O_{23} > 0.5$ .

### 2.1. Calibration based on O II recombination lines

Peimbert, Storey, & Torres-Peimbert (1993) were the first to determine O/H values for gaseous nebulae based on the recombination coefficients for O II lines computed by Storey (1994). The temperature dependence of the O II lines is relatively weak and very similar to that of the H I lines, therefore the  $O^{++}/H^+$  ratios are independent of the electron temperature. Alternatively the  $O^{++}/H^+$  ratios derived

from collisionally excited lines do depend strongly on the average temperature,  $T_0$ , and the mean temperature square,  $t^2$  (e. g.: Peimbert 1967, Peimbert & Costero 1969, Ruiz et al. 2003, Peimbert et al. 2004).

In H II regions the recombination lines typically yield abundances higher than the optical collisionally excited lines by factors in the 2 to 3 range, if a value of  $t^2 = 0.00$  is adopted. This difference is due to the presence of strong temperature variations that yield  $t^2$  values in the 0.02 to 0.06 range. The  $t^2$  determinations have been obtained by three different methods: a) by comparing the temperature derived from the intensity ratio of the Balmer continuum to a recombination Balmer line with  $T(4363)$  (Peimbert 1967), b) by determining  $T_0$  and  $t^2$  from a least squares method using the line intensities of a large number of He I lines (Peimbert, Peimbert, & Ruiz 2000, Peimbert, Peimbert, & Luridiana 2002), and c) by computing the  $t^2$  value needed to derive the same  $N(O^{++})/N(H)$  ratio from O II recombination lines and [O III] collisionally excited lines (Peimbert, Storey, & Torres-Peimbert 1993). For the best observed objects the three methods yield the same result, within the errors, supporting the presence of large temperature variations (e. g. Peimbert 2003; Peimbert et al. 2004, 2005; Esteban et al. 2005). The presence of temperature variations affect strongly the  $T(4363)$  method, weakly the *PIM* method, and leave the O II<sub>RL</sub> method unaffected, or in other words the O II<sub>RL</sub> method is independent of the temperature structure of the nebula.

In Table 1 we present the O/H values derived from the O II<sub>RL</sub> method and the  $T(4363)$  method for H II regions of nearby galaxies and the Galaxy. The  $N(O^{++})/N(H^+)$  values were derived from the O II recombination lines. Most of the  $N(O^+)/N(H^+)$  values were derived from  $I(3727)$  together with  $T(5755/6584)$  and the  $t^2$  value determined from several methods, while the rest were derived from O I recombination lines. In the first column we list the object, in the second column the O/H value based on the O II<sub>RL</sub> method, in the third column the O/H value based on the  $T(4363)$  method, in the fourth column the  $\log O_{23}$  observed value, and in the fifth column the ionization parameter  $P$  defined as  $P \equiv I([\text{O III}]\lambda\lambda 4959, 5007)/I([\text{O II}]\lambda 3727 + [\text{O III}]\lambda\lambda 4959, 5007)$  (Pilyugin 2001). The average fraction of oxygen twice ionized in the sample presented in Table 1 amounts to 68%.

In Figure 1 we present the data of Table 1 and the calibration of Pagel's indicator provided by the O II<sub>RL</sub> method and the  $T(4363)$  method. Pilyugin

TABLE 1

O/H VALUES DERIVED BY THE O II<sub>RL</sub> AND THE T(4363) METHODS

Object	O/H		log $O_{23}$	$P$	Ref.
	O II <sub>RL</sub>	$T(4363)$			
M16	8.81	8.56	0.58	0.27	1
M8	8.71	8.51	0.53	0.38	2
M17	8.76	8.52	0.73	0.83	2
M17	8.87	8.56	0.75	0.84	3
M20	8.71	8.53	0.60	0.20	1
NGC 3576	8.86	8.56	0.78	0.78	4
NGC 3576	8.73	8.52	0.79	0.79	3
Orion	8.71	8.51	0.77	0.86	5
Orion	8.61	8.47	0.74	0.84	6
NGC 3603	8.72	8.46	0.89	0.92	1
S 311	8.57	8.39	0.72	0.32	7
NGC 5461	8.81	8.56	0.80	0.74	8
N11B(LMC)	8.74	8.41	0.80	0.70	3
NGC 604	8.66	8.49	0.67	0.70	8
30 Doradus	8.57	8.34	0.89	0.86	3
30 Doradus	8.54	8.33	0.90	0.85	9
N66 (SMC)	8.47	8.11	0.90	0.85	3
NGC 5253	8.39	8.18	0.97	0.85	10
NGC 6822	8.37	8.08	0.90	0.88	11
NGC 2363	8.20	7.87	1.00	0.97	8

Given in  $12 + \log O/H$ .

1- García-Rojas et al. (2006a); 2- García-Rojas et al. (2006b); 3- Tsamis et al. (2003); 4- García-Rojas et al. (2004); 5- Esteban et al. (2004); 6- Esteban et al. (1998); 7- García-Rojas et al. (2005); 8- Esteban et al. (2002); 9- Peimbert (2003); 10- López-Sánchez et al. (2006, zones A and B); 11- Peimbert et al. (2005).

(2001) has found that the  $O_{23}$  indicator depends strongly on the ionization parameter  $P$  and that for a given  $O_{23}$  value the higher the  $P$  value the higher the O/H value. The amount of objects with measured O II recombination line intensities or accurate  $t^2$  values is very small and it is not possible to produce an absolute calibration for different  $P$  values, but of the 20 objects in Table 1 sixteen present  $0.70 < P < 0.97$ , and based on them we have produced a calibration for  $P = 0.8$ . In these calibrations we have also made use of the four objects with  $0.20 < P < 0.38$  including the relative increase in O/H predicted by the  $T(4363)$  method for a change from  $P = 0.3$  to  $P = 0.8$ , that amounts to  $\sim 0.2$  dex (Pilyugin & Thuan 2005).

There are three aspects that need to be considered in future work to have a full calibration of the  $O_{23}$  indicator independent of temperature variations:

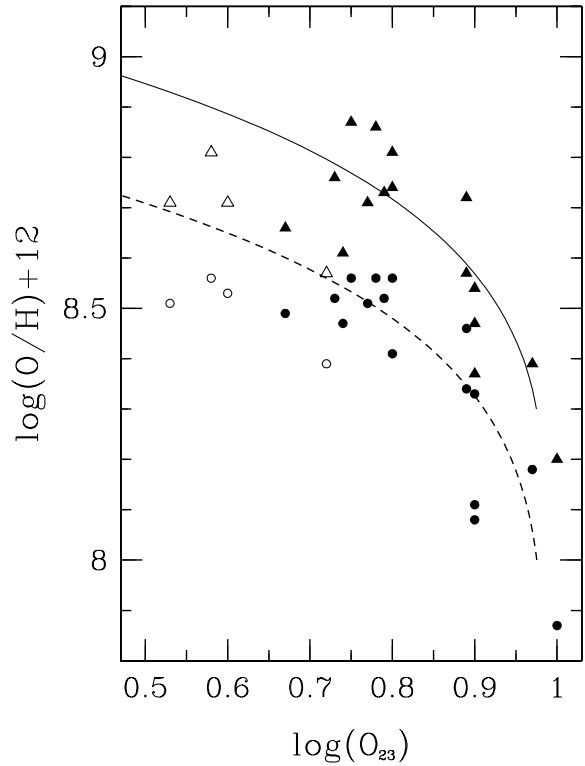


Fig. 1. Pagel's  $O_{23}$  abundance indicator calibrated using abundances determined with recombination lines — O II<sub>RL</sub> method (triangles and solid line) —, and abundances determined with collisionally excited lines and  $t^2 = 0.00$  —  $T(4363)$  method (circles and dotted line) —. The data is presented in Table 1. The filled symbols correspond to objects with  $0.70 < P < 0.97$  and the empty symbols to objects with  $0.20 < P < 0.38$ . The lines indicate the calibrations for  $P = 0.8$ . To include the  $0.20 < P < 0.38$  objects in the  $P = 0.8$  calibrations we have added to them 0.2 dex in the O/H axis based on the relative difference with  $P$  found by Pilyugin and Thuan (2005).

a) the calibration of the high metallicity branch for  $O_{23} < 0.5$ , b) the calibration of the  $O_{23}$  low metallicity branch, and c) the variation of the O ionization degree at a given  $O_{23}$  value. We will say a few words about these aspects.

To calibrate the  $O_{23}$  indicator for values of  $\log O_{23} < 0.5$  in the high metallicity branch we need additional observations of O II lines. In general the higher the metallicity the lower the degree of ionization and the lower the  $N(O^{++})/N(O)$  ratio. Therefore when most of the O becomes  $O^+$  the O II recombination lines become very weak and can not be used to derive the O/H values, consequently we need other temperature indicators to estimate  $T_0$

and  $t^2$ . For example the combination of good Balmer continuum temperatures with temperatures derived from the  $\lambda\lambda 5755, 6584$  [N II] lines. Good Balmer continuum temperatures are difficult to determine due to the underlying stellar contribution that contaminates the nebular continuum emission.

It is not possible with present day equipment to calibrate the  $O_{23}$  indicator for the low metallicity branch with O II recombination lines because they become weaker as  $N(O)/N(H)$  decreases. Fortunately due to the higher  $T(4363)$  values in this branch the effect of the temperature variations on the  $N(O)/N(H)$  determinations becomes smaller, and we expect differences between the  $T(4363)$  and the  $PIM$  methods to become smaller than  $\sim 0.2$  dex. Moreover the effect due to the temperature structure might be estimated by deriving  $T_0$  and  $t^2$  from the  $T(4363)$  and  $T(\text{HeI})$  temperatures (Peimbert et al. 2000, 2002).

In general for giant very bright H II regions in the  $O_{23}$  low metallicity branch and in the high metallicity branch for  $\log O_{23} > 0.5$  most of the O is twice ionized; but for old H II regions and those ionized by a handful of O stars the fraction of O once ionized becomes important. To test the effect of the ionization degree in our calibration it is necessary to obtain abundances of H II regions at a given  $O_{23}$  with different O ionization degrees.

### 2.2. Calibrations based on photoionization models

The  $PIM$  method is based on photoionization models where O/H is an input of the models and the observed  $O_{23}$  values are adjusted to the predicted ones. Calibrations based on this method have been presented by many authors (e. g.: McCall, Rybski, & Shields 1985; Dopita, & Evans 1986; McGaugh 1991; Zaritsky, Kennicutt & Huchra 1994; Kewley, & Dopita 2002; Kobulnicky, & Kewley 2004). The  $PIM$  method depends on the quality of the models. A good model for the ionizing cluster should include: an initial mass function, the time elapsed since the beginning of the star formation, and a star formation rate; while for the nebula it should include the gaseous density distribution.

Photoionization models not yet include all the physical processes needed to reproduce all the emission line ratios observed in real nebulae. For example they do not include the possible presence of stellar winds due to WR stars nor the possible presence of supernova remnants and related shocks. From a study of NGC 604, a giant extragalactic H II region in M33, Yang et al. (1996) conclude that the velocity width of the  $H\alpha$  line consists of equal contributions from thermal broadening, stellar winds and

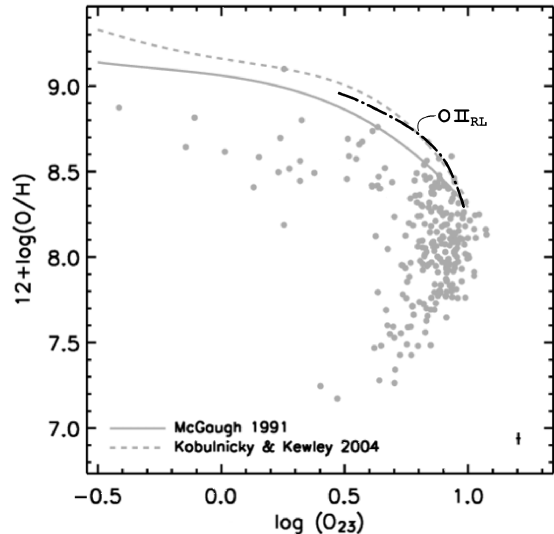


Fig. 2. Our O II<sub>RL</sub> calibration for  $P = 0.8$  superimposed to a slide by J. Moustakas presented at the workshop on "Bright Line Abundance Calibrations at Low and High Metallicities" (Minneapolis, May 2005). The dots represent O/H ratios determined from the observed  $T(4363)$  values under the assumption of  $t^2 = 0.00$ , they are compared with the  $PIM$  calibrations by McGaugh (1991) and Kobulnicky & Kewley (2004). The O II<sub>RL</sub> calibration for  $P = 0.8$  is in very good agreement with the  $PIM$  calibrations.

SNRs, and gravity. Even the best photoionization models, those tailored to fit I Zw 18, NGC 2363, and NGC 346, predict  $T(4363)$  values smaller than observed (Stasińska & Schaerer 1999; Luridiana, Peimbert, & Leitherer 1999, and Relaño, Peimbert, & Beckman 2002), probably indicating the need for additional heating sources. Photoionization models typically predict  $t^2 \approx 0.005$ , values considerably smaller than those derived from observations that are typically in the  $0.02 < t^2 < 0.06$  range.

In Figure 2 we present our O II<sub>RL</sub> calibration for  $P = 0.8$  and compare it with the calibrations based on the  $PIM$  method by McGaugh (1991) and Kobulnicky & Kewley (2004). The agreement between the O II<sub>RL</sub> and the  $PIM$  calibrations is very good because the  $PIM$  calibrations do not fit the  $\lambda 4363$  line intensity, which depends strongly on  $T_0$  and  $t^2$ , they do fit the  $\lambda\lambda 5007$  and  $3727$  line intensities that show a much smaller dependence on  $T_0$  and  $t^2$  than the  $\lambda 4363$  line intensity.

### 2.3. Calibrations based on observations of $O_{23}$ and $T_e(4363)$

The  $T(4363)$  method is based on adjusting the observed  $O_{23}$  values with the abundances derived

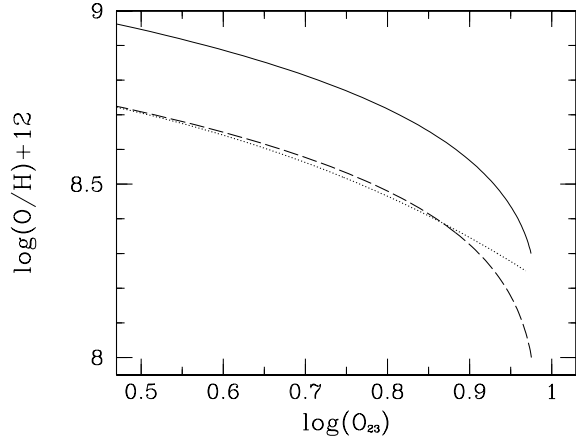


Fig. 3. Comparison of three absolute calibrations for  $P = 0.8$ . The solid line represents our  $O\ II_{RL}$  calibration, the dashed line represents our  $T(4363)$  calibration, and the dotted line the Pilyugin and Thuan (2005) calibration. Note the excellent agreement between the  $T(4363)$  calibrations, this agreement implies that the sole difference between our  $O\ II_{RL}$  calibration and the  $T(4363)$  calibration by Pilyugin and Thuan is due to temperature variations inside the observed objects.

from  $T(4363)$  under the assumption that  $t^2 = 0.00$ . The calibrations based on this method depend strongly on the temperature structure of the nebulae and underestimate the O/H values by factors of about 2 to 3 because  $\lambda\ 4363$  has a large Boltzmann factor for collisional excitation that depends strongly on  $T_0$  and  $t^2$ .

The differences between the  $O\ II_{RL}$  calibration and the observed values derived with the  $T(4363)$  calibration for  $t^2 = 0.00$  presented in Figure 3 are in the 0.2 to 0.3 dex range and are similar to the differences presented in Table 1, therefore we attribute most of the difference between the  $O\ II_{RL}$  and the  $T(4363)$  calibrations as being due to temperature variations over the observed volumes. Moreover from the similarity shown in Figure 2 between the  $PIM$  calibration and the  $O\ II_{RL}$  calibration for  $P = 0.8$  we also conclude that the main difference between the  $PIM$  calibration and the  $T(4363)$  calibration is due to temperature variations over the observed volume.

In their recent calibration of the  $T(4363)$  method for different  $P$  values, Pilyugin and Thuan (2005) adopted the temperature for the once ionized O region given by  $T(O^+) = 0.7 \times T(4363) + 3000$  K (Garnett 1992) to derive the  $N(O^+)/N(H^+)$  ratios. Therefore the  $T(O^+)$  and the  $N(O^+)/N(H^+)$  values so derived also depend on the possible presence of temperature variations in the  $O^{++}$  regions.

In Table 2 we present the averaged O/H determi-

TABLE 2  
AVERAGE O/H VALUES FOR 14 DISK GALAXIES

Method	$\langle O/H \rangle$ $\rho = 0$	$\langle O/H \rangle$ $\rho = 0.4\rho_{25}$	$\langle \text{Gradient} \rangle$ $\text{dex}\rho_{25}^{-1}$	Cal.
<i>PIM</i>	9.14	8.86	-0.48	1
<i>T(4363)</i>	8.58	8.38	-0.28	2

Results by Moustakas & Kennicutt (2006), O/H values given in  $12 + \log O/H$ .

1- McGaugh(1991); 2- Pilyugin, & Thuan (2005).

nations by Moustakas & Kennicutt (2006) based on  $O_{23}$  observations of 234 H II regions using the  $PIM$  calibration by McGaugh (1991) and the  $T(4363)$  calibration by Thuan and Pilyugin (2005). The galactocentric distance is given by  $\rho$ , the O/H value at  $\rho = 0$  corresponds to the extrapolation to the galactic center, and  $\rho_{25}$  is the radius of the semi-major axis at the  $B_{25}$  mag arc sec $^{-2}$  isophote. For this sample the abundance controversy amounts to 0.56 dex for  $\rho = 0$ , and to 0.48 dex for  $\rho = 0.4\rho_{25}$ . The increase in the O/H difference with metallicity between both calibrations, as well as the steeper abundance gradient for the  $PIM$  calibration relative to the  $T(4363)$  calibration are consistent with the idea that temperature variations are mainly responsible for these differences. The larger differences at larger O/H values are expected due to the higher sensitivity of O/H on  $T_0$  and  $t^2$  as  $T(4363)$  becomes smaller, in other words the larger differences are due to the Boltzmann factor for collisional excitation of the  $\lambda\ 4363$  line that becomes larger at smaller  $T(4363)$  values.

### 3. GALACTIC H II REGIONS AND THE SOLAR ABUNDANCES

In addition to the evidence presented in section 2.1 in favor of large  $t^2$  values, and consequently in favor of the  $O\ II_{RL}$  method, there is another independent test that can be used to discriminate between the  $T(4363)$  method and the  $O\ II_{RL}$  method that consists in the comparison of stellar and H II region abundances of the solar vicinity. To carry out this comparison we have added 0.08 dex to all the gaseous O/H determinations to take into account the estimated fraction of O tied up in dust grains in H II regions (see Esteban et al. 1998).

Esteban et al. (2005) determined that  $12 + \log(O/H) = 8.77$  for the ISM of the solar vicinity based on the O/H galactic gradient derived from the  $O\ II_{RL}$  method. Alternatively from the solar ratio by Asplund, Grevesse, & Sauval (2005), that amounts to  $12 + \log(O/H) = 8.66$ , and taking into account the

increase of the O/H ratio due to galactic chemical evolution since the Sun was formed, that according to state of the art chemical evolution models of the Galaxy amounts to 0.13 dex (e.g. Carigi et al. 2005), we obtain an O/H value of 8.79 dex, in excellent agreement with the value based on the O II<sub>RL</sub> method. In this comparison we are assuming that the solar abundances are representative of the abundances of the solar vicinity ISM when the Sun was formed.

There are two other determinations of the present O/H value in the ISM that can be made from observations of F and G stars of the solar vicinity. According to Allende-Prieto et al. (2004) the Sun appears deficient by roughly 0.1 dex in O, Si, Ca, Sc, Ti, Y, Ce, Nd, and Eu, compared with its immediate neighbors with similar iron abundances, by adding this 0.1 dex difference to the solar value by Asplund et al. (2005) we obtain a lower limit of  $12 + \log \text{O/H} = 8.76$  for the local interstellar medium. A similar result is obtained from the data by Bensby & Feltzing (2005) who obtain for the six most O-rich thin-disk F and G dwarfs of the solar vicinity an average  $[\text{O/H}] = 0.16$ ; by adopting their value as representative of the present day ISM of the solar vicinity we find  $12 + \log \text{O/H} = 8.82$ . Both results are in excellent agreement with the O/H value derived from the O II<sub>RL</sub> method.

On the other hand, based on the  $T(4363)$  method with  $t^2 = 0.00$  Deharveng et al. (2000) and Pilyugin, Ferrini, & Shkvarun (2003) obtain  $12 + \log \text{O/H}$  values of 8.61 and 8.60 respectively for the solar vicinity, values about 0.2 dex smaller than the stellar predictions and the value derived from the O II<sub>RL</sub> method.

#### 4. CALIBRATION OF OTHER METALLICITY INDICATORS

There are other O/H indicators that have been proposed in the literature:  $O_3N_2 \equiv I([\text{O III}]\lambda 5007/I([\text{N II}]\lambda 6584))$ , presented by Alloin et al. (1979),  $N_2 \equiv I([\text{N II}]\lambda 6584)/I(\text{H}\alpha)$ , presented by Storchi-Bergmann et al. (1994),  $S_{23} \equiv I([\text{S II}]\lambda\lambda 6717, 6731 + [\text{S III}]\lambda 9069)/I(\text{H}\alpha)$ , presented by Vílchez, & Esteban (1996),  $Ar_3O_3 \equiv I([\text{Ar III}]\lambda 7135/I([\text{O III}]\lambda 5007))$ , and  $S_3O_3 \equiv I([\text{S III}]\lambda 9069/I([\text{O III}]\lambda 5007))$ , these two proposed by Stasińska (2006). Since these indicators are calibrated with models that fit the nebular O/H lines, or with O/H determinations based on  $T(4363)$  observations, the absolute calibration shift derived for the  $O_{23}$  calibration based on the O II<sub>RL</sub> method also applies to them. Therefore the O/H values derived from them have to be increased, as is the

case for the  $O_{23}$  indicator, if they are calibrated with the  $T(4363)$  method.

In addition to the absolute calibration shift the  $N_2$  indicator has other problems: a) it shows a larger dispersion than the other indicators making it less reliable (e. g. Stasińska 2006), b) according to Stasińska (2006) and Moustakas and Kennicutt (2006) the possible contribution to the  $I([\text{N II}]\lambda 6584)/I(\text{H}\alpha)$  ratio by the extended low density interstellar medium, that is expected to be more important for galaxies farther away, also might produce a bias in the calibration of the  $N_2$  indicator, c) the indicators based on O, S, and Ar have the advantage that these are primary elements formed by massive stars, therefore their relative abundance ratios are almost constant during the chemical evolution of galaxies, this is not the case for N that is produced by two types of stars, massive (that end their lives as supernovae) and low and intermediate mass stars (that end their lives as white dwarfs), and in two different ways from C and O produced by their own star (primary origin), or using C and O of the progenitor cloud where the star formed (secondary origin); moreover, other effects, as stellar rotation (Meynet & Maeder 2002) and the treatment of hot bottom burning, cause substantial differences in the computed N yields (see the compilation by Gavilán, Mollá, & Buell 2006).

If the  $N_2$  or the  $O_3N_2$  indicators based on observations of nearby galaxies, are used for objects at large distances, considering that we are comparing two sets of different ages, the variation in N/O as a function of time predicted by the chemical evolution models for galaxies of different masses and different star formation histories has to be considered.

#### 5. CONCLUSIONS

The O II<sub>RL</sub> method supports the suggestion that the controversy produced by the relatively high O/H values predicted by the *PIM* calibrations and the relatively low O/H values predicted by the  $T(4363)$  calibrations are mainly due to temperature variations.

The best way to calibrate the  $O_{23}$  indicator is to use the O II<sub>RL</sub> method to obtain the O/H values because it is independent of the temperature structure.

The use of  $T(4363)$  values to derive O/H, under the assumption of constant temperature, provides a lower limit to the O/H abundance ratios.

Since the nebular lines are less sensitive to  $T_0$  and  $t^2$  than the auroral lines, the model calibrations that adjust the nebular lines are closer to the O II<sub>RL</sub> calibration than those derived using the observed  $T(4363)$  values.

For a given object the O II recombination lines provide gaseous abundances that are about 0.2 to 0.3 dex higher than those derived from collisionally excited lines and  $T(4363)$  under the assumption that  $t^2 = 0.00$ .

By using the O II recombination lines to derive O/H abundances in Galactic H II regions together with state of the art Galactic chemical evolution models we obtain an excellent agreement with the O/H solar value derived by Asplund et al.(2005). We also find an excellent agreement between the H II region O/H abundances derived from recombination lines and those derived from young G dwarfs, this comparison is independent of Galactic chemical evolution effects since both types of objects correspond to the present abundances in the ISM of the solar vicinity.

With the O II<sub>RL</sub> calibration and observations of emission line galaxies at different  $z$  values it will be possible to study the chemical evolution of the universe as a whole. All the other O/H indicators, like those known as  $O_3N_2$ ,  $N_2H\alpha$ ,  $S_{23}$ ,  $Ar_3O_3$ , and  $S_3O_3$ , depend on an absolute calibration and we recommend to calibrate them using the O II<sub>RL</sub> method.

Models of the chemical evolution of N/O versus O/H as a function of time for different types of galaxies are required to calibrate the  $N_2$  and  $O_3N_2$  indicators.

We need more high resolution observations of O II recombination lines in the local universe to refine and extend the O II<sub>RL</sub> calibration. We need objects with  $\log O_{23}$  smaller than 0.5 in the high metallicity branch. We also need objects of different  $P$  values at a given  $O_{23}$  value in the high metallicity branch.

It is a pleasure to acknowledge fruitful discussions with Evan Skillman, Bob Kennicutt, Henry Lee, and Valentina Luridiana. MP is grateful to our Florida colleagues for their warm hospitality during this meeting.

## REFERENCES

- Allende-Prieto, C., Barklem, P. S., Lambert, D. L., & Cunha, K. 2004, *A&A*, 420, 183
- Alloin, D., Collin-Souffrin, S., Joly, M., & Vigroux, L. 1979, *A&A*, 78, 200
- Asplund, M., Grevesse, N., & Sauval, A. J. 2005, in: *Cosmic Abundances as Records of Stellar Evolution and Nucleosynthesis*, ed. F. N. Bash, & T. G. Barnes, ASP Conference Series, 25
- Bensby, T., & Feltzing, S. 2006, *MNRAS*, 367, 1181
- Campbell, A. 1988, *ApJ*, 335, 644
- Carigi, L., Peimbert, M., Esteban, C., & García-Rojas, J. 2005, *ApJ*, 623, 213
- Castellanos, M., Díaz, A. I., & Terlevich, E. 2002, *MNRAS*, 329, 315
- Deharveng, L., Peña, M., Caplan, J., & Costero, R. 2000, *MNRAS*, 311, 329
- Dopita, M. A., & Evans, I. N. 1986, *ApJ*, 307, 431
- Edmunds, M. G., & Pagel, B. E. J. 1984, *MNRAS*, 211, 507
- Esteban, C., Peimbert, M., García-Rojas, J., Ruiz, M. T., Peimbert, A., & Rodríguez, M. 2004, *MNRAS*, 355, 229
- Esteban, C., García-Rojas, J., Peimbert, M., Peimbert, A., Ruiz, M. T., Rodríguez, M., & Carigi, L. 2005, *ApJ*, 618, L95
- Esteban C., Peimbert M., Torres-Peimbert S., & Escalante V. 1998, *MNRAS*, 295, 401
- Esteban, C., Peimbert, M., Torres-Peimbert, S., & Rodríguez, M. 2002, *ApJ*, 581, 241
- García-Rojas, J., Esteban, C., Peimbert, A., Peimbert, M., Rodríguez, M., & Ruiz, M. T. 2005, *MNRAS*, 362, 301
- García-Rojas, J., Esteban, C., Peimbert, M., Costado, M. T., Rodríguez, M., Peimbert, A., & Ruiz, M. T. 2006a, *MNRAS*, 368, 253
- García-Rojas, J., Esteban, C., Peimbert, A., Rodríguez, M., Peimbert, M., & Ruiz, M. T. 2006b, *RMAA*, submitted
- García-Rojas, J., Esteban, C., Peimbert, M., Rodríguez, M., Ruiz, M. T., & Peimbert, A. 2004, *ApJS*, 153, 501
- Garnett, D. R. 1992, *AJ*, 103, 1330
- Gavilán, M., Mollá, M., & Buell, J. F. 2006, *A&A*, 450, 509
- Kewley, L. J., & Dopita, M. A. 2002, *ApJS*, 142, 35
- Kobulnicky, H. A., Kennicutt, R. C., & Pizagno, J. L. 1999, *ApJ*, 514, 544
- Kobulnicky, H. A., & Kewley, L. J. 2004, *ApJ*, 617, 240
- López-Sánchez, A. R., Esteban, C., García-Rojas, J., Peimbert, M., & Rodríguez, M. 2006, *ApJ*, submitted
- Luridiana, V., Peimbert, M., & Leitherer, C. 1999, *ApJ*, 527, 110
- McCall, M. L., Rybski, P. M., & Shields, G. A. 1985, *ApJS*, 57, 1
- McGaugh, S. S. 1991, *ApJ*, 380, 140
- Meynet, G., & Maeder, A. 2002, *A&A*, 390, 561
- Moustakas, J., & Kennicutt, R. C. 2006, in press, *astro-ph/0511731*
- Pagel, B. E. J., Edmunds, M. G., Blackwell, D. E., Chun, M. S., & Smith G. 1979, *MNRAS*, 189, 95
- Peimbert, A. 2003, *ApJ*, 584, 735
- Peimbert, A., & Peimbert, M. 2005, *RevMexAA*, SC, 23, 9
- Peimbert, A, Peimbert, M. & Luridiana, V. 2002, *ApJ*, 565, 668
- Peimbert, A., Peimbert, M., & Ruiz, M. T. 2005, *ApJ*, 634, 1056
- Peimbert, M. 1967, *ApJ*, 150, 825
- Peimbert, M., & Costero, R. 1969, *Bol. Obs. Tonantzintla y Tacubaya*, 5, 3

- Peimbert, M., & Peimbert, A. 2003, *RevMexAA*, SC, 16, 113
- Peimbert, M., Peimbert, A., & Ruiz M. T. 2000, *ApJ*, 541, 688
- Peimbert, M., Peimbert, A., Ruiz, M. T., & Esteban, C. 2004, *ApJS*, 150, 431, 2004
- Peimbert, M., Storey, P. J., & Torres-Peimbert, S. 1993, *ApJ*, 414, 626
- Pilyugin, L. S. 2000, *A&A*, 362, 325
- Pilyugin, L. S. 2001, *A&A*, 369, 594
- Pilyugin, L. S. 2003, *A&A*, 399, 1003
- Pilyugin, L. S., Ferrini, F., & Shkvarun, R. V. 2003, *A&A*, 401, 557
- Pilyugin, L. S., & Thuan, T. X. 2005, *ApJ*, 631, 231
- Relaño, M., Peimbert, M., & Beckman, J. 2002, *ApJ*, 564, 704
- Roy, J.-R., Belley, J., Dutil, Y., & Martin, P. 1996, *ApJ*, 460, 284
- Ruiz, M. T., Peimbert, A., Peimbert, M., & Esteban, C. 2003, *ApJ*, 595, 247
- Stasińska, G. 2006, *A&A*, 454, L127
- Stasińska, G., & Schaerer, D. 1999, *A&A*, 351, 72
- Storchi-Bergmann, T., Calzetti, D., & Kinney, A. L. 1994, *ApJ*, 429, 572
- Storey, P. J. 1994, *A&A*, 282, 999
- Torres-Peimbert, S., Peimbert, M., & Fierro, J. 1989, *ApJ*, 345, 186
- Tsamis, Y. G., Barlow, M. J., Liu, X.-W., Danziger, I. J., & Storey, P. J. 2003, *MNRAS*, 338, 687
- Vílchez, J. M., & Esteban, C. 1996, *MNRAS*, 280, 720
- Yang, H., Chu, Y.-H., Skillman, E. D., & Terlevich, R. 1996, *AJ*, 112, 146
- Zaritsky, D., Kennicutt, R. C., & Huchra, J. P. 1994, *ApJ*, 420, 87